Electronic Supplementary Material (ESI) for Nanoscale.

Stabilizing zinc anode via tunable covalent organic frameworks-based solid electrolyte interphase

Vipada Aupama[1], Wathanyu Kao-ian[1], Jinnawat Sangsawang[1], Gopalakrishnan Mohan[1], Suttipong Wannapaiboon[2], Ahmad Azmin Mohamad[3], Prasit Pattananuwat[4,5], Chakrit Sriprachuabwong[6], Wei-Ren Liu[7], Soorathep Kheawhom[1,5,8,*]

[1] Department of Chemical Engineering, Faculty of Engineering, Chulalongkorn University, Bangkok 10330, Thailand

[2] Synchrotron Light Research Institute, 111 University Avenue, Muang District, Nakhon Ratchasima 30000, Thailand

[3] School of Materials and Mineral Resources Engineering, Universiti Sains Malaysia, Nibong Tebal, Pulau Pinang 14300, Malaysia

[4] Department of Materials Science, Faculty of Science, Chulalongkorn University, Bangkok 10330, Thailand

[5] Center of Excellence on Advanced Materials for Energy Storage, Chulalongkorn University, Bangkok 10330, Thailand

[6] National Science and Technology Development Agency, Pathumthani 12120, Thailand

[7] Department of Chemical Engineering, Research Center for Circular Economy, Chung Yuan Christian University, Chung Li, Taiwan (R.O.C.)

[8] Bio-Circular-Green-economy Technology & Engineering Center (BCGeTEC), Faculty of Engineering, Chulalongkorn University, Bangkok 10330, Thailand

**Corresponding author: soorathep.k@chula.ac.th*

Section	
S-1	**Field emission scanning electron microscope (FE-SEM)**
S-2	**Powder X-ray diffraction (PXRD) spectra of COF powder**
S-3	**X-ray photoelectron spectroscopy (XPS)**
S-4	**Electrochemical performance**
S-5	**Methodology reported in the literature for protective layer focus on Zn anode**

S-1: Field emission scanning electron microscope (FE-SEM)

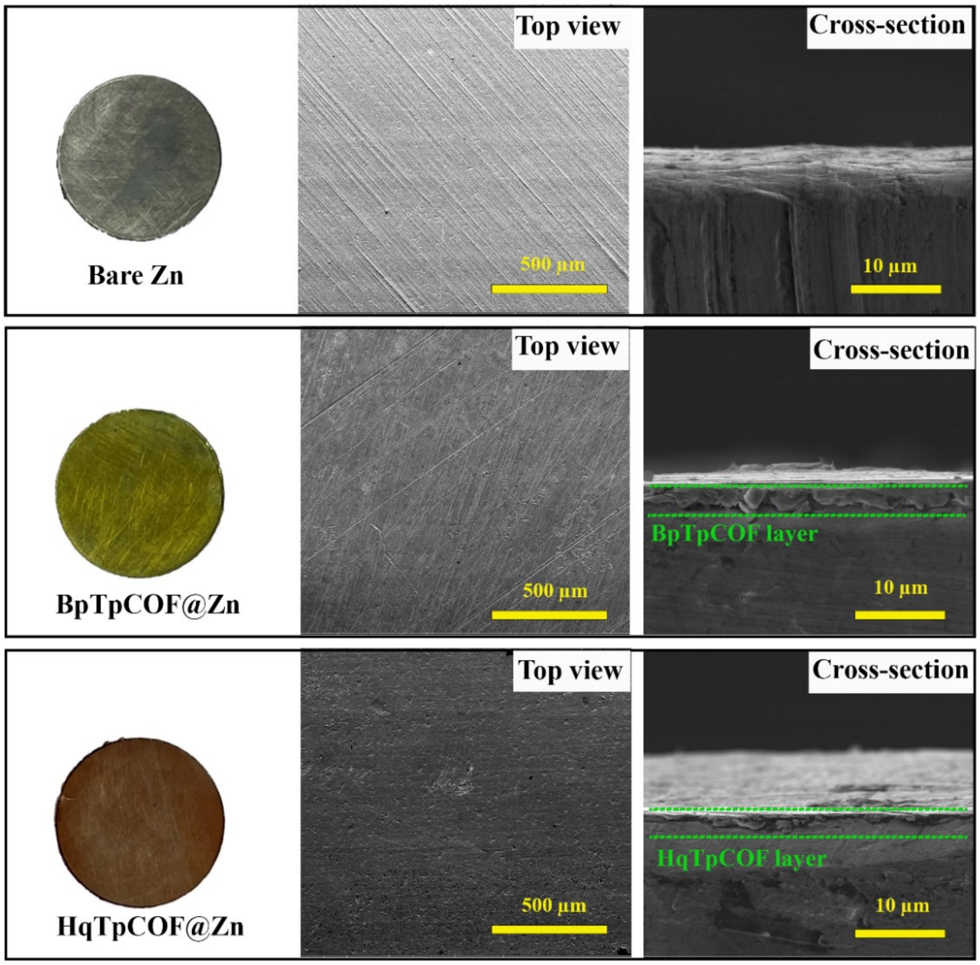

Figure S1. FE-SEM images of the samples.

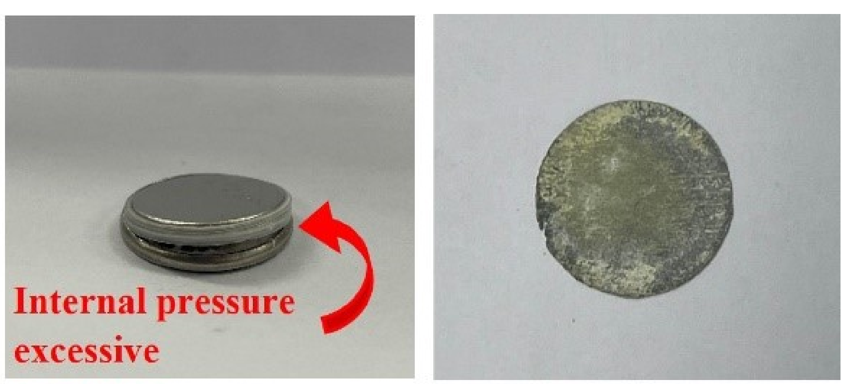

Figure S2. The BpTpCOF@Zn cell and BpTpCOF@Zn electrode after the battery failed.

S-2: Powder X-ray diffraction (PXRD) spectra of COF powder

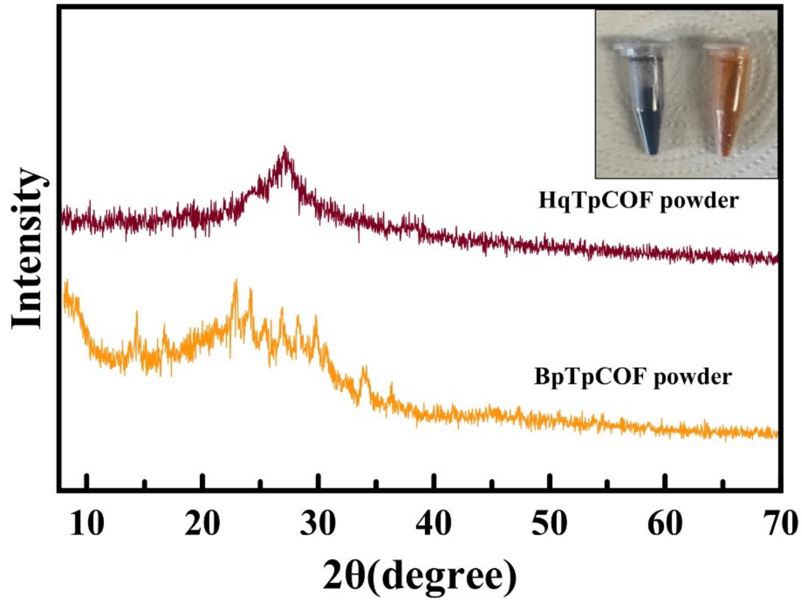

Figure S3. PXRD spectra of HqTpCOF and BpTpCOF powder.

PXRD spectra were used to characterize COF's structure. The conditions were used: 40 kV, 15 mA, step size: 0.02°. In Fig.S2, two COFs' power demonstrates a broader peak around 2θ = 27º. This peak broadening can be ascribed to π-π stacking between benzene rings in the COF layer. The resultant PXRD pattern is compared to the literature [1, 2].

S-3: X-ray photoelectron spectroscopy (XPS)

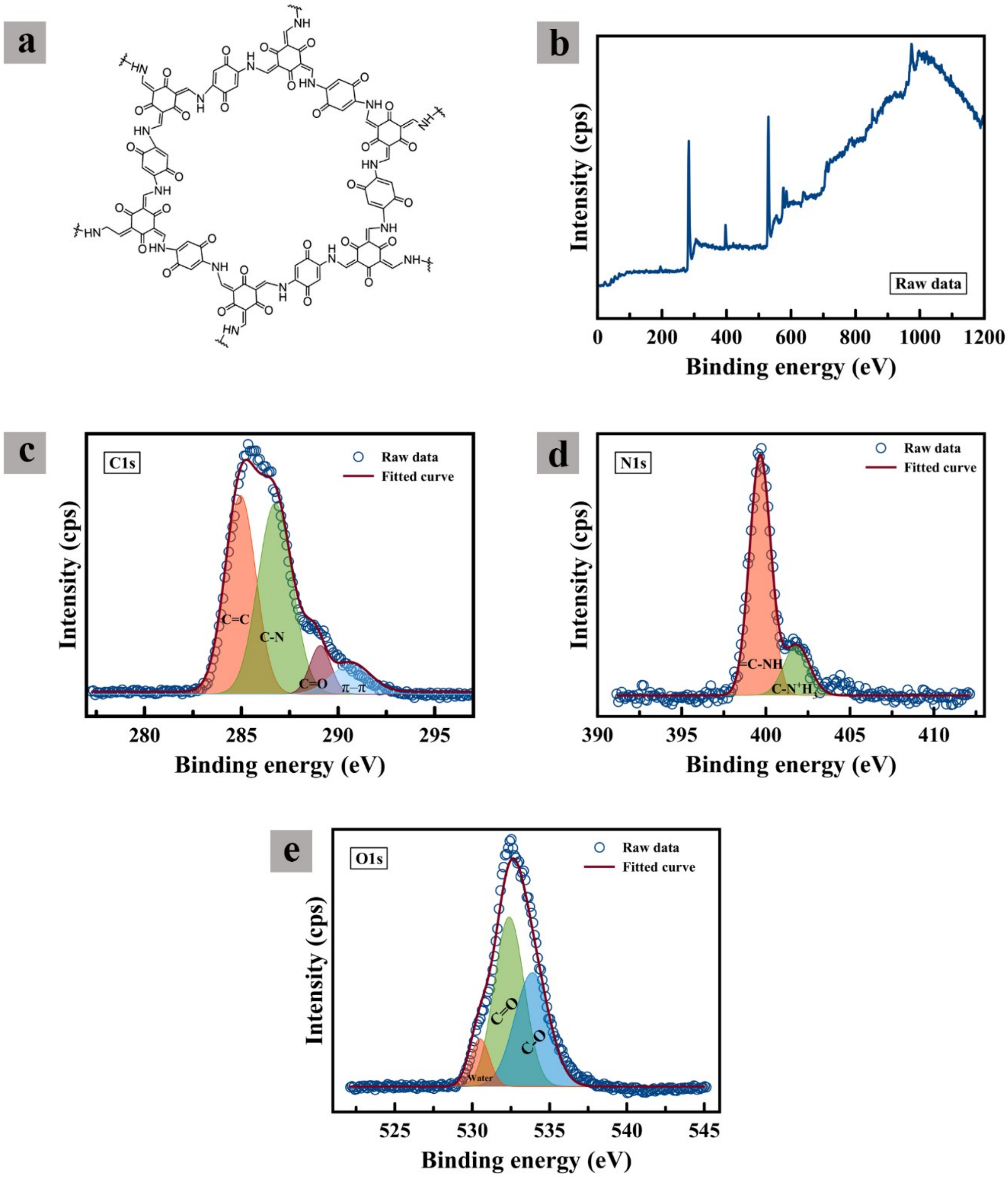

Figure S4. Schema of XPS spectra: a) Molecular scheme of HqTpCOF, b) Raw data, c) C 1s, d) N 1s, and e) O 1s peaks.

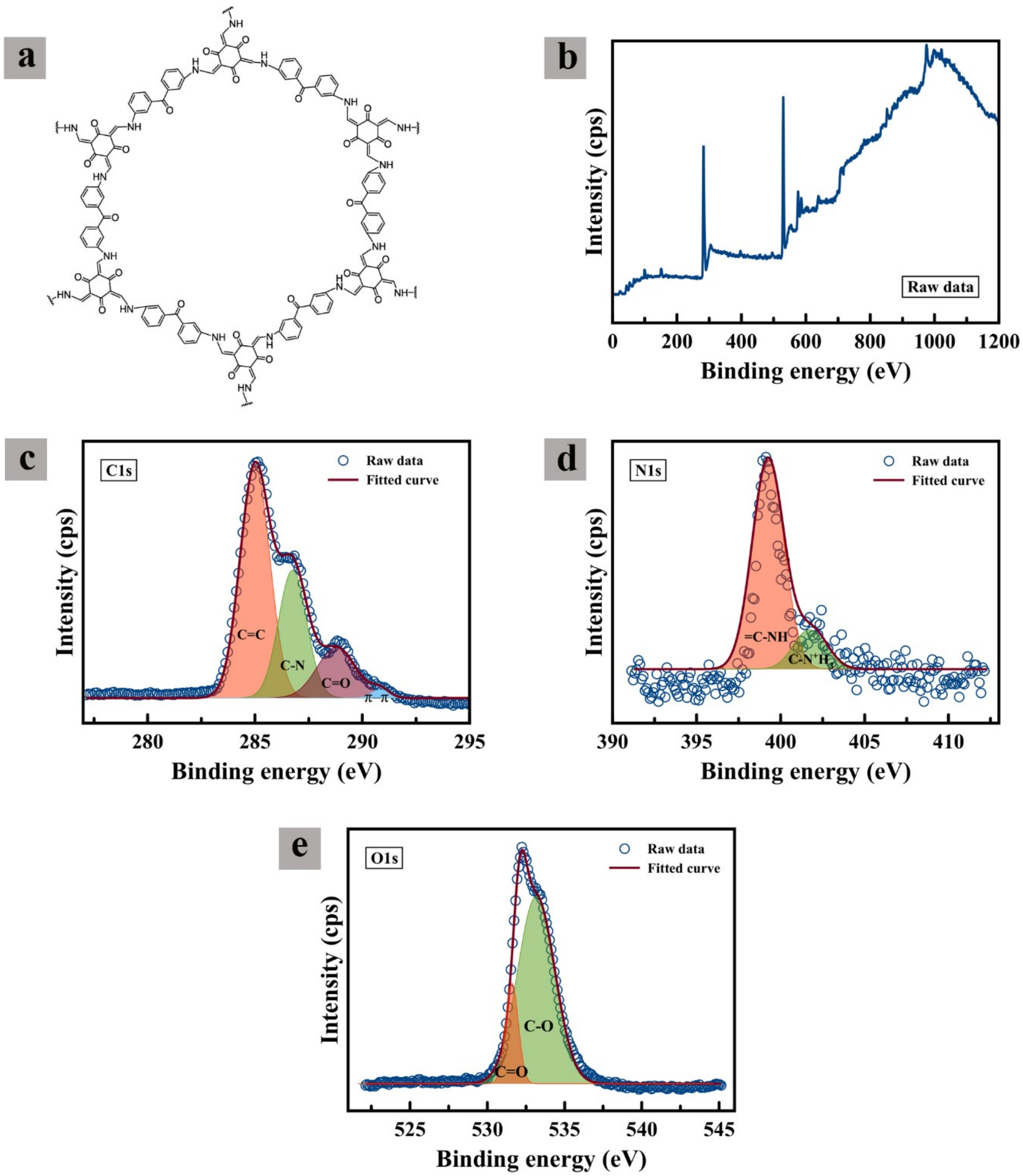

Figure S5. Schema of XPS spectra: a) Molecular scheme of BpTpCOF, b) Raw data, c) C 1s, d) N 1s, and e) O 1s peaks.

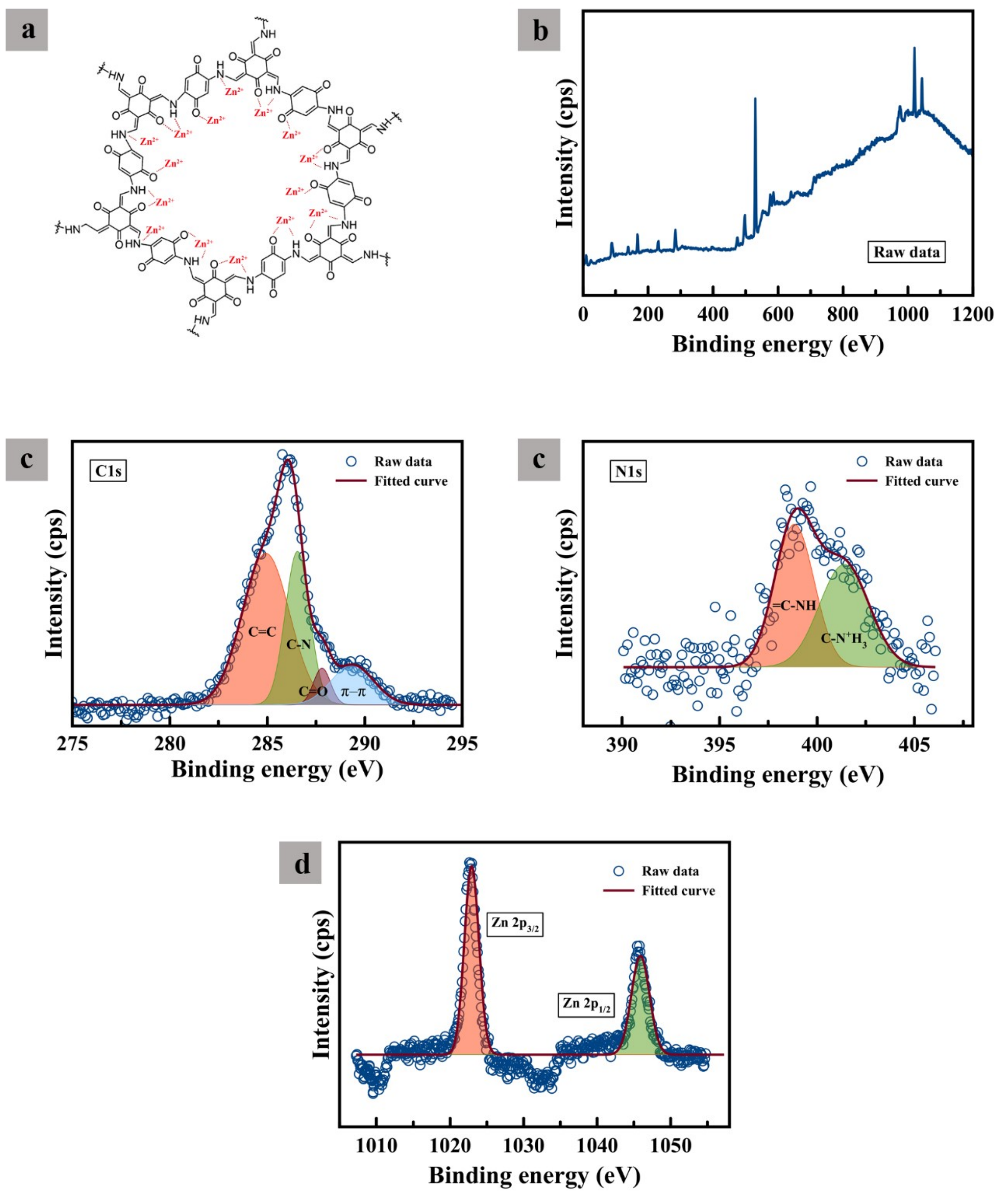

Figure S6. Schema of XPS spectra soaking in electrolyte: a) Molecular scheme of HqTpCOF, b) Raw data, c) C 1s, d) N 1s, and e) Zn 2p peaks.

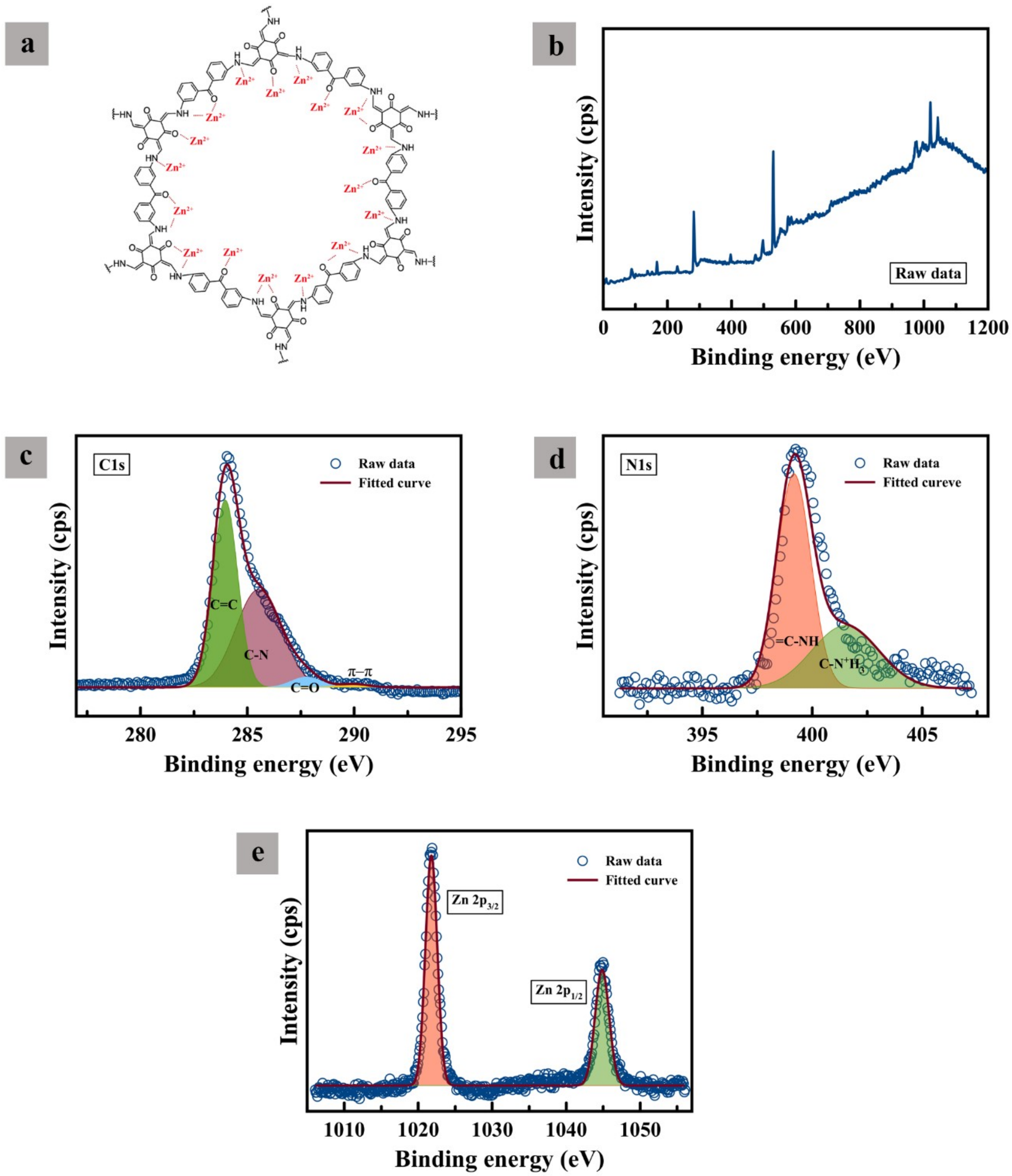

Figure S7. Schema of XPS spectra after soaking in electrolyte: a) Molecular scheme of BpTpCOF, b) Raw data, c) C 1s, d) N 1s, and e) Zn 2p peaks.

Table S1. The deconvoluted XPS profiles of C1s

No.	Conditions	Binding energy				Area under graph				Percentage			
		Peak C-C	Peak C-N	Peak C=O	Peak π–π	C-C	C-N	C=O	π–π	%C-C	%C-N	%C=O	% π–π
1	**BpTpCOF -pristine**	285	286.5	288.5	290.79	5801.933	4377.373	1673.126	306.1569	47.7188	36.00231	13.76086	2.51803
2	**BpTpCOF -soaked**	285	286.5	288.5	290.79	14251.53	8596.927	988.8445	91.96462	59.5569	35.92641	4.132365	0.384319
3	**HqTpCOF -pristine**	285	286.5	288.5	290.79	7855.073	8435.065	1324.448	1481.096	41.13534	44.17263	6.93585	7.756185
4	**HqTpCOF -soaked**	285	286.5	288.5	290.79	1952.297	1818.996	170.7408	461.0557	44.33925	41.31181	3.877749	10.47118

Table S2. The deconvoluted XPS profiles of N1s

No.	Condition	Binding energy		Area under graph		Percentage	
		Peak =C-NH	Peak N^+	=C-NH	N^+	% =C-NH	%N^+
1	**BpTpCOF -pristine**	399.1	401.7	763.2618	143.1326	84.20857	15.79143
2	**BpTpCOF -soaked**	399.1	401.7	890.9019	511.2319	63.53901	36.46099
3	**HqTpCOF -pristine**	399.1	401.7	1670.409	428.9245	79.56853	20.43147
4	**HqTpCOF -soaked**	399.1	401.7	230.3591	208.3899	52.50362	47.49638

S-4: The effects of thickness of COFs films

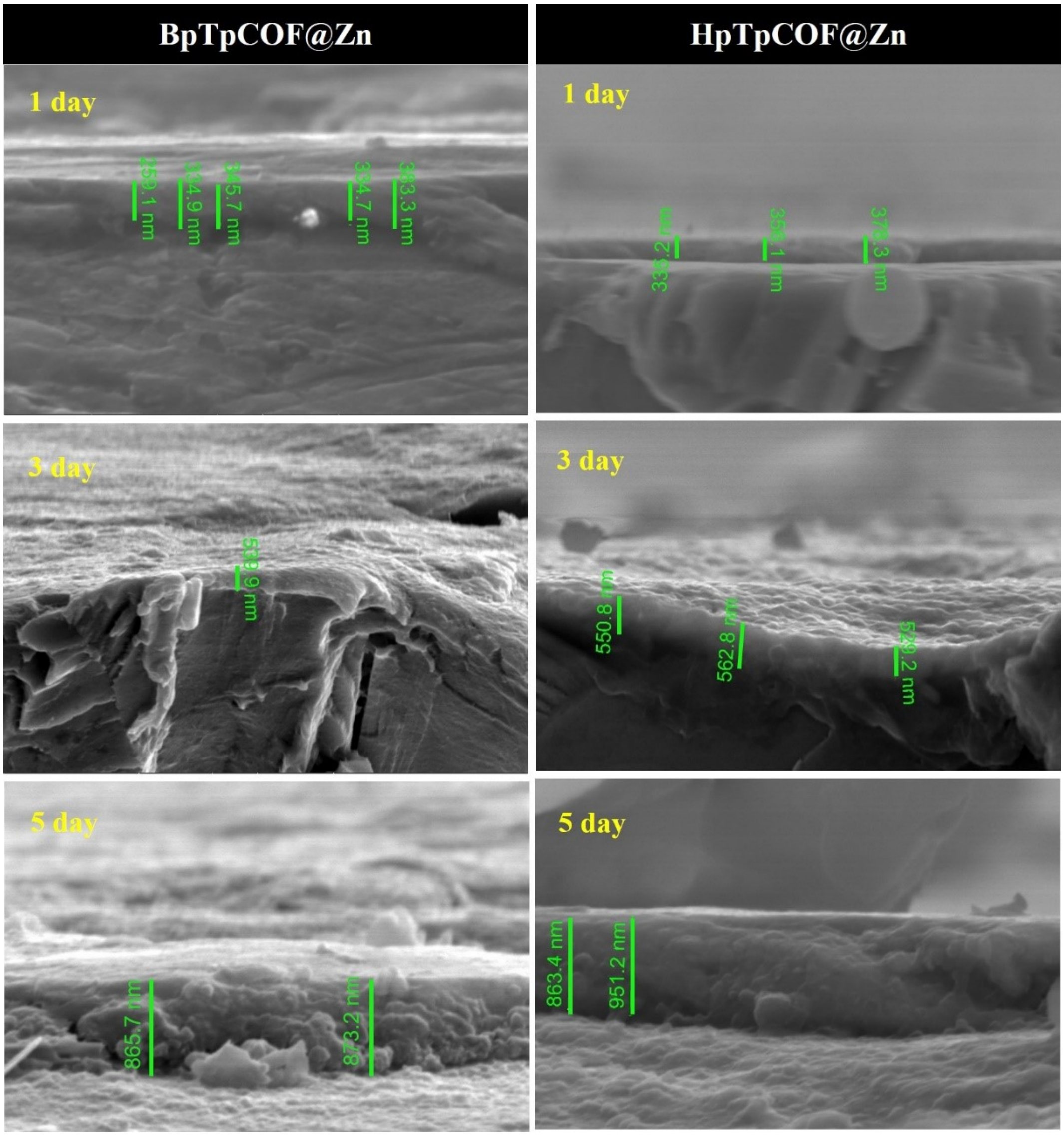

Figure S8. The thickness of the COFs layer at various times to dip.

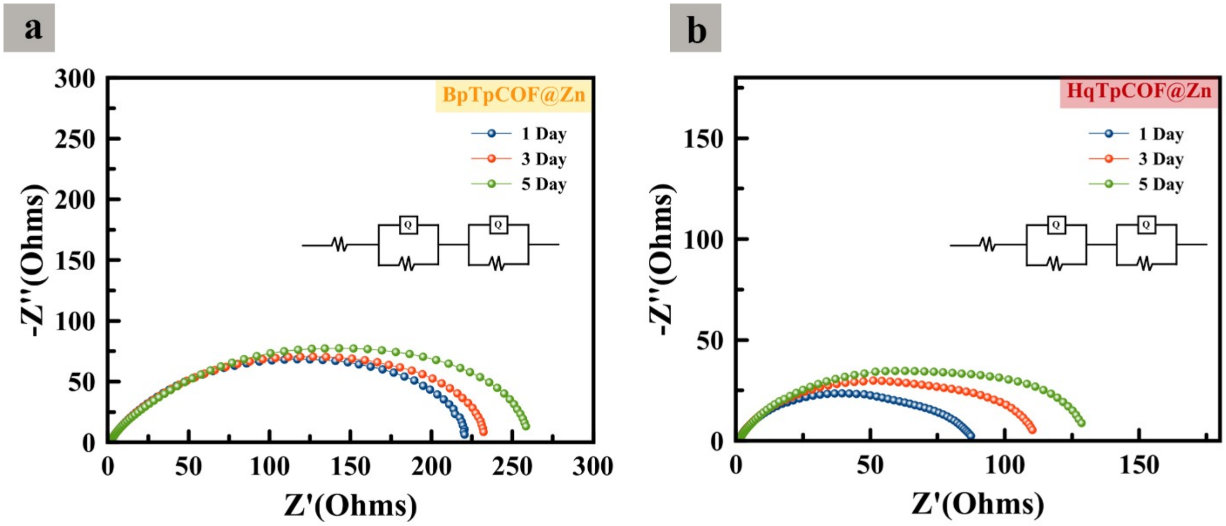

Figure S9. EIS plot for different electrodes at various COFs layer thicknesses: a) BpTpCOF@Zn and b) HqTpCOF@Zn.

Table S3. Resistance of the BpTpCOF@Zn anode at various thickness layers of COFs: Fitted with the equivalent circuit as shown in Fig. S9a.

Duration	SEI resistance (R_{COF})(Ω)	Charge transfer resistance (R_{ct})(Ω)
1 Day	42.24	184
3 Day	52.44	190.1
5 Day	59.27	213.9

Table S4. Resistance of the HqTpCOF@Zn anode at various thickness layers of COFs: Fitted with the equivalent circuit as shown in Fig. S9b.

Duration	**SEI resistance (R_{COF})(Ω)**	**Charge transfer resistance (R_{ct})(Ω)**
1 Day	11.5	77.64
3 Day	27.58	89.27
5 Day	36.1	97.06

S-5: Electrochemical performance

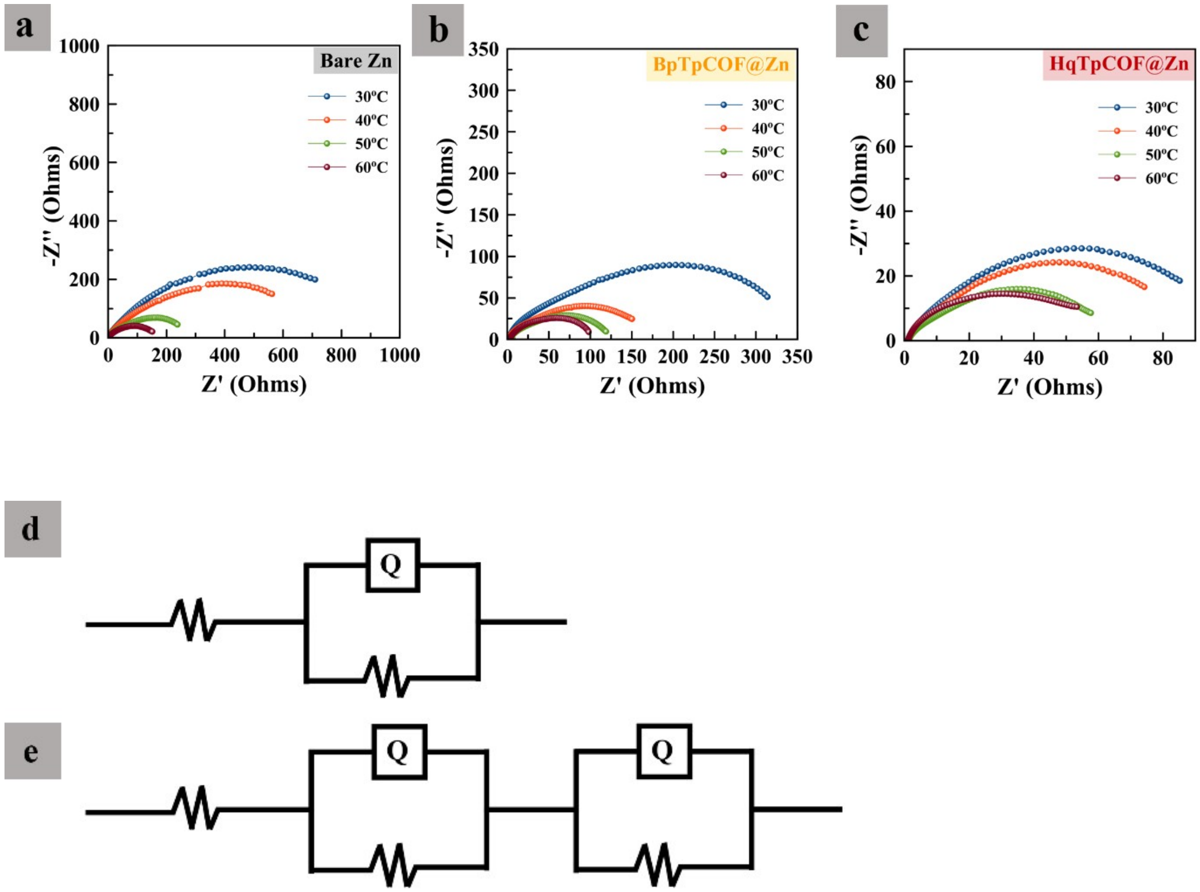

Figure S10. EIS images: a) Nyquist plots of bare Zn symmetrical cells at various temperatures, b) Nyquist plots of BpTpCOF@Zn symmetrical cells at various temperatures, c) Nyquist plots of HqTpCOF@Zn symmetrical cells at various temperatures, d) Equivalent circuit model: bare Zn electrode, and e) Equivalent circuit model: COFs@Zn electrodes.

Table S5. Charge-transfer resistance (R_{ct}) of the different anodes at various temperatures: equivalent circuit as shown in Figs. S10a-c .

Temperature (^oC)	Charge-transfer resistance (Ω)		
	Bare Zn	BpTpCOF@Zn	HqTpCOF@Zn
30	913.3	299.4	78.83
40	605.1	139.8	63.73
50	226.4	108	55.96
60	136.4	73.79	32.52

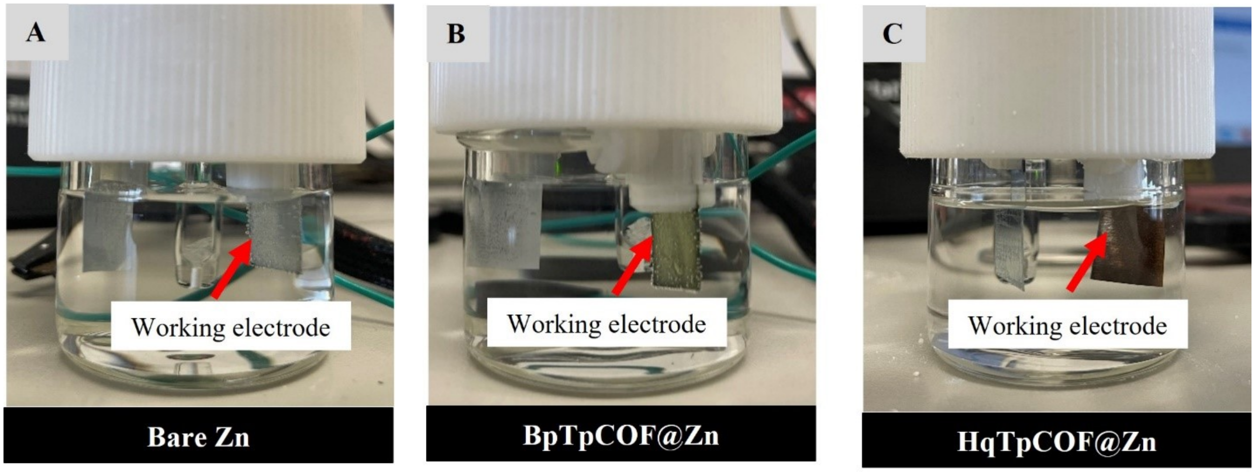

D

Sample	Corrosion potential, E_{corr}(mV)	Corrosion current, I_{corr}(mA)
Bare Zn	-973	7.92
BpTpCOF@Zn	-970	7.77
HqTpCOF@Zn	-953	7.2

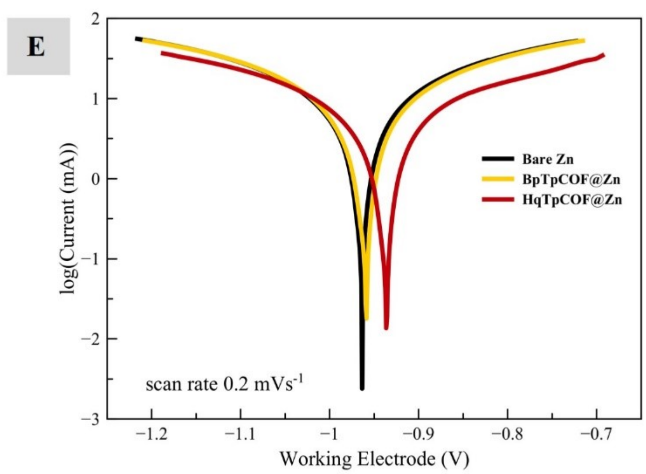

Figure S11. Linear polarization test.

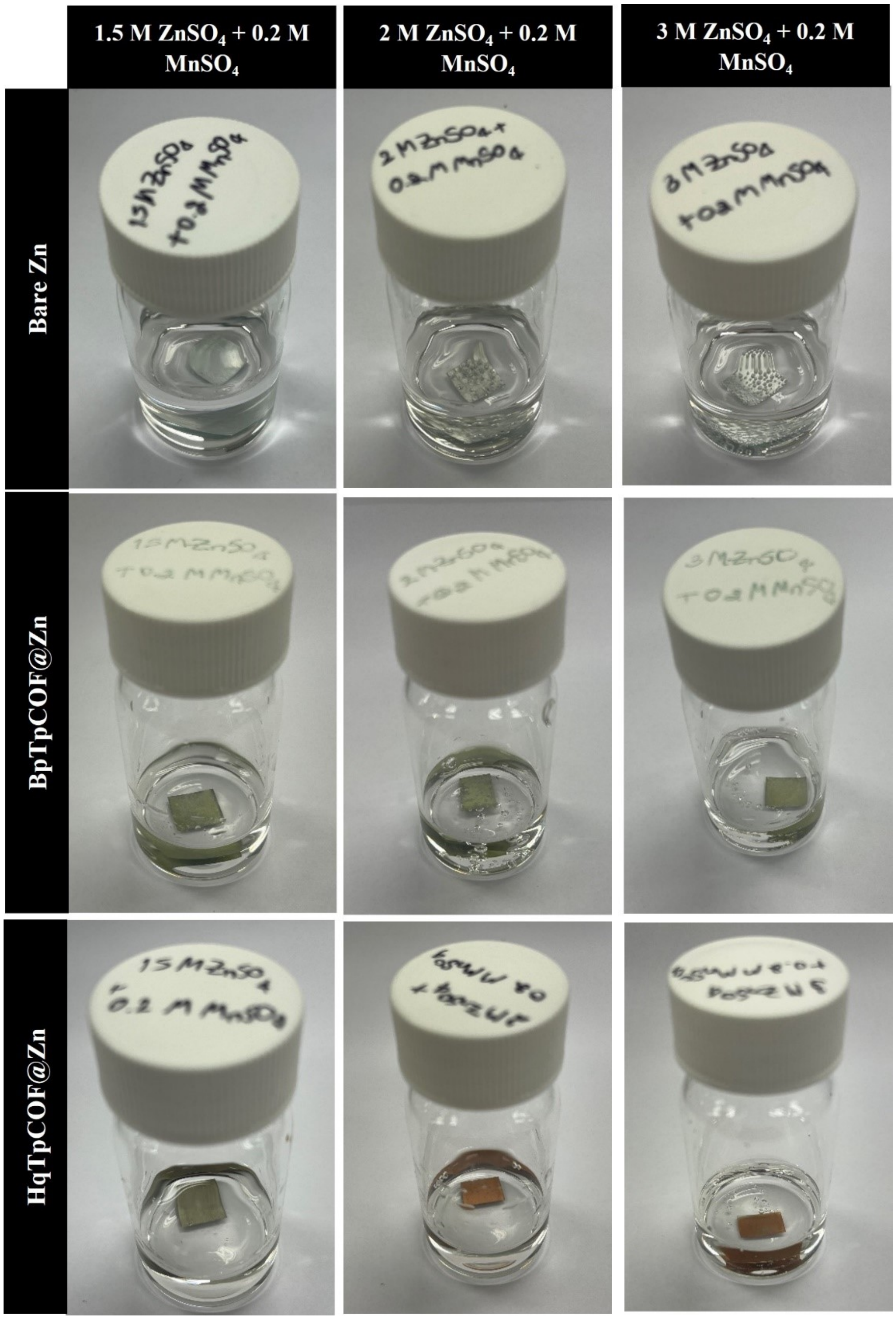

Figure S12. Images of different Zn electrodes in various concentrations of electrolytes: 1.5 M $ZnSO_4$+ 0.2 M $MnSO_4$, 2 M ZnSO4+0.2 M $MnSO_4$, and 3 M $ZnSO_4$+0.2 M $MnSO_4$ in 14 days.

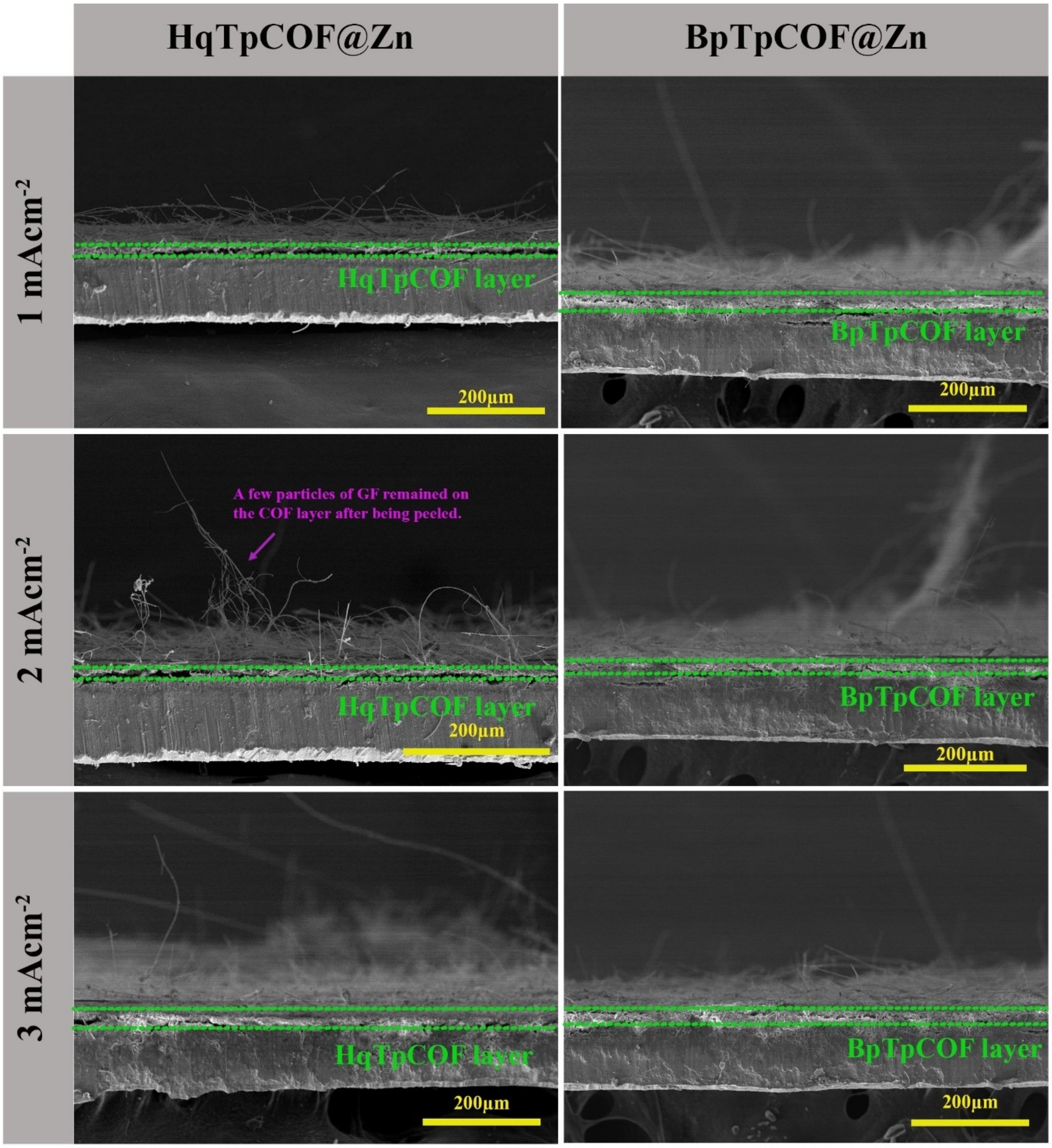

Figure S13. Cross-section of Zn anodes: Bare Zn, BpTpCOF@Zn, and HqTpCOF@Zn from symmetrical cells after 100 cycles at various current densities (1, 2, and 3 mA cm^{-2}).

S-4: Methodology reported in the literature for Metal/Covalent organic frameworks layer: focus on Zn anode

	Materials	Processing Method	Electrolytes	Current density	Areal Capacity	Voltages polarization	Cycling performance	Ref.
MOFs	ZIF-8	In situ growth	2M $ZnSO_4$	0.5 mA cm^{-2}	0.2 mAh cm^{-2}	~70 mV	>680 h	3
	ZIF-11	Doctor blading	2M $ZnSO_4$	0.4 mA cm^{-2}	0.2 mAh cm^{-2}	-	>740 h	4
				0.5 mA cm^{-2}	0.2 mAh cm^{-2}	-	>620 h	
				1 mA cm^{-2}	0.5 mAh cm^{-2}	-	>555 h	
	$Zn(TFSI)_2$-TFEP@MOF	-	1 M $Zn(TFSI)_2$-TFEP@MOF/H_2O	0.5 mA cm^{-2}	0.5 mAh cm^{-2}	~20 mV	>700 h	5
COFs	DAAQ-TFP COF	Dip-coating	2M $ZnSO_4$	1 mA cm^{-2}	1 mAh cm^{-2}	~36 mV	>420 h	1
				2 mA cm^{-2}		~40 mV	>270 h	
	TpPa-SO_3H	Transfer	1M $ZnSO_4$	1 mA cm^{-2}	5 mAh cm^{-2}	~81 mV	>1000 h	6
	HqTpCOF@Zn	**Dip-coating**	**2M $ZnSO_4$ + 0.2 M $MnSO_4$**	**1 mA cm^{-2}**	**1 mAh cm^{-2}**	**~39 mV**	**>700 h**	**This work**
	BpTpCOF@Zn					**~55 mV**	**>300 h**	

Table S6. Comparison of performance between this work and other MOFs/COFs as protective layers at symmetric cell configuration.

References

1. J. H. Park, M.-J. Kwak, C. Hwang, K.-N. Kang, N. Liu, J.-H. Jang and B. A. Grzybowski, *Adv. Mater.*, 2021, **33**, 2101726, doi: 10.1002/adma.202101726.
2. S. Kandambeth, B. P. Biswal, H. D. Chaudhari, K. C. Rout, S. Kunjattu H., S. Mitra, S. Karak, A. Das, R. Mukherjee, U. K. Kharul and R. Banerjee, *Adv. Mater.*, 2017, **29**, 1603945, doi: 10.1002/adma.201603945.
3. M. Cui, B. Yan, F. Mo, X. Wang, Y. Huang, J. Fan, C. Zhi and H. Li, *Chem. Eng. J.*, 2022, **434**, 134688, doi: 10.1016/j.cej.2022.134688.
4. M. He, C. Shu, A. Hu, R. Zheng, M. Li, Z. Ran and J. Long, *Energy Storage Materials*, 2022, **44**, 452-460, doi: 10.1016/j.ensm.2021.11.010.
5. Z. Li, L. Ye, G. Zhou, W. Xu, K. Zhao, X. Zhang, S. Hong, T. Ma, M.-C. Li, C. Liu and C. Mei, *Chem. Eng. J.*, 2023, **457**, 141160, doi: 10.1016/j.cej.2022.141160.
6. J. Zhao, Y. Ying, G. Wang, K. Hu, Y. D. Yuan, H. Ye, Z. Liu, J. Y. Lee and D. Zhao, *Energy Storage Materials*, 2022, **48**, 82-89, doi: 10.1016/j.ensm.2022.02.054.